Approaching disorder-free transport in high mobility conjugated polymers

Deepak Venkateshvaran[1*], Mark Nikolka[1*], Aditya Sadhanala[1], Vincent Lemaur[2], Mateusz Zelazny[1], Michal Kepa[3], Michael Hurhangee[4], Auke Jisk Kronemeijer[1], Vincenzo Pecunia[1], Iyad Nasrallah[1], Igor Romanov[1], Katharina Broch[1], Iain McCulloch[4], David Emin[5], Yoann Olivier[2], Jerome Cornil[2], David Beljonne[2] and Henning Sirringhaus[1]

[1]Optoelectronics Group, Cavendish Laboratory, JJ Thomson Avenue, Cambridge CB3 0HE, United Kingdom.

[2]Laboratory for Chemistry of Novel Materials, Université de Mons, 20 Place du Parc, 7000 Mons, Belgium.

[3]Centre for Science at Extreme Conditions, University of Edinburgh, Mayfield Road, Edinburgh EH9 3JZ, United Kingdom

[4]Department of Chemistry and Centre for Plastic Electronics, Imperial College London, London SW7 2AZ, United Kingdom.

[5]Department of Physics and Astronomy, University of New Mexico, 1919 Lomas Blvd NE, Albuquerque, NM 87131, USA.

[*]equal contribution

Conjugated polymers are enabling flexible semiconductor devices that can be processed from solution at low temperatures. Over the last 25 years, devices' performances have improved greatly as a wide variety of molecular structures have been studied [1]. However, one major limitation has not been overcome; transport properties in polymer films are still limited by pervasive conformational and energetic disorder [2-5]. This not only limits the rational design of materials with higher performance, but also prevents study of physical phenomena

associated with an extended π-electron delocalization along the polymer backbone. Here we report a comparative transport study of several high mobility conjugated polymers by field-effect modulated Seebeck, transistor and sub-bandgap optical absorption measurements. We show that in several of these polymers, most notably in a recently reported, indacenodithiophene-based donor-acceptor copolymer with near amorphous microstructure [6], the charge transport properties are approaching intrinsic disorder-free limits in which all molecular sites are thermally accessible. Molecular dynamics simulations identify the origin of this long sought-after regime as a planar, torsion-free backbone conformation that is surprisingly resilient to side chain disorder. Our results provide important molecular-design guidelines for "disorder-free" conjugated polymers.

In several donor-acceptor co-polymers [7-10] surprisingly high field-effect mobilities > 1cm^2/Vs have recently been reported despite the microstructure of these polymers being less ordered than that of (semi)crystalline polymers, such as poly-3-hexylthiophene (P3HT) [3] or poly(2,5-bis(3-alkylthiophen-2-yl)thieno(3,2-b)thiophene) (PBTTT) [5], and in some cases near-amorphous. The high mobilities have been attributed to a network of tie chains providing interconnecting transport pathways between crystalline domains [3], but this does not fully explain how these polymers can exhibit significantly *higher* mobilities than P3HT/PBTTT. To probe energetic disorder in these systems we investigate the Seebeck coefficient α, that can be determined experimentally by measuring the electromotive force that develops across a material in response to an applied temperature differential ΔT; $\alpha = $ emf/ΔT. For small carrier concentration, as in the herein-reported experiments, the dominant contribution to α is the entropy of mixing associated with adding a carrier into the density of states, which is determined by the density of thermally accessible transport states [11-14]. If the energetic dispersion is less than kT the density of thermally accessible states will be temperature independent and equal to the density of molecular sites. By contrast, if the energetic dispersion among hopping sites is much greater than kT the density of thermally accessible states will increase as the temperature is raised. Thus we can estimate the energetic disorder relative to

kT associated with transport by measuring the temperature dependence of the Seebeck coefficient of FETs which independently control the carrier density [15].

We have investigated a range of state-of-the-art DPP and isoindigo copolymers and show results here for PSeDPPBT [16, 17] and DPPTTT [18-19] with mobilities of 0.3-0.5 cm^2/Vs and 1.5-2.2 cm^2/Vs, respectively. PBTTT serves as a (semi)crystalline polymer reference system. Among the many polymers we investigated we find the lowest degree of energetic disorder in indacenodithiophene-co-benzothiadiazole (IDTBT). IDTBT is a highly soluble polymer (Supplementary Information (SI) section 1) exhibiting high field-effect mobilities despite a lack of long range crystalline order [6, 20]. Top-gate IDTBT FETs with films annealed at 100 °C and Cytop gate dielectric reliably exhibit near-ideal performance: a low threshold voltage of V_{Th} = −3 V, a low contact resistance [Fig. 1(a)] and a high saturation mobility of 1.5-2.5 cm^2/Vs extracted from a near ideal, quadratic current dependence on gate voltage.

It may be necessary to comment on why these mobility values are lower than the highest values claimed in the literature [9, 10, 18]. On the one hand there is ongoing debate about possible overestimation of mobilities in polymer FETs due to non-idealities in their electrical characteristics [21]. All mobility values reported here were conservatively estimated. Contact resistance related artefacts make it possible, for example, to extract up to an order of magnitude higher mobilities from non-optimized IDTBT devices with non-ideal electrical characteristics (SI section 2). On the other hand we have restricted ourselves to top-gate FETs with spin-coated films and not used techniques for enhancing interfacial orientation / alignment over that present in the bulk that may enhance mobilities for certain materials [10]. This enables us to correlate interface-sensitive FET/Seebeck measurements with bulk-sensitive optical spectroscopy.

Among the polymers investigated IDTBT had not only one of the highest mobilities, if not the highest, but also the most ideal electrical characteristics (SI section 2). This is evident in the temperature-dependent drain current I_D versus gate voltage V_G characteristics in the saturation regime which were fit to $I_D \propto (V_G - V_{Th})^\gamma$ between 200 and 300 K. For IDTBT the exponent γ equals the ideal,

temperature-independent value of 2 [Fig. 1(b)]. By contrast, γ rises with decreasing temperature as $\gamma = (T_0/T) + 1$ for PBTTT, PSeDPPBT and DPPTTT, which is commonly observed in polymer FETs and interpreted in terms of carriers hopping within an exponential density of states with characteristic width $kT_0 > kT$ [22]. Concomitantly the mobility rises upon increasing the magnitude of the gate voltage as trap states within the band-tail are progressively being filled (SI section 2). In contrast to the other polymers this disorder model does not fit the IDTBT FET data even when T_0 is taken as small as 330 K. We know of no prior report of such ideal ($\gamma = 2$) behavior for a polymer FET. The IDTBT transfer characteristics are well fit over the entire temperature range with a disorder-free, MOSFET-like model with a thermally activated, but gate-voltage independent mobility [Fig. 1(c)]. This was confirmed by extracting directly the gate voltage dependence of the mobility from the transfer characteristics of devices with patterned semiconductor layer to minimize leakage and fringe currents. In IDTBT the mobility was nearly independent of gate voltage for $|V_G| > 20$ V across the entire temperature range, while in PBTTT the mobility strongly increases with gate voltage at lower temperatures [Fig. 1(d)]. These results suggest that energetic disorder is significantly lower in IDTBT than in the other polymers.

To accurately measure Seebeck coefficients of FETs with a 20-50 μm channel length as functions of gate voltage and temperature, we developed a micro-fabricated device architecture with an integrated heater and temperature sensors positioned along the FET's channel [23] (SI section 3). The carrier concentrations n in the accumulation layer were estimated from capacitance versus gate voltage measurements (SI section 4). We find Seebeck coefficients (Fig. 2) that are (1) much larger than $k/e \approx 86$ μV/K, (2) decreasing functions of increasing carrier concentration n and (3) independent of temperature between 200-300 K within the measurement error. Temperature-independent Seebeck coefficients over a similar temperature range have been reported previously only for single crystals of the molecular semiconductors pentacene and rubrene [15].

We have attempted to interpret the Seebeck and FET measurements as a function of temperature consistently in terms of the variable-range hopping disorder

model used in Ref. [24], that is akin to models used for explaining analogous measurements in amorphous silicon [25]. For PBTTT and PSeDPPBT this may be possible, but the fits depend on several unknown parameters and, as discussed above, the disorder model breaks down for IDTBT (SI Section 2). A simpler, more consistent interpretation of the three salient Seebeck features that is applicable to all polymers is a narrow-band model in which charge carriers experience a small degree of energetic disorder and are able to access a temperature independent density of thermally accessible sites. The narrowness of the carriers' energy bands is likely due to polaron formation [14] as supported by charge accumulation spectroscopy (SI section 5 and 6). In the simplest narrow-band model the Seebeck coefficient can be expressed as the sum of three contributions (SI section 7, [14]):

$$\alpha = \frac{k}{e} \ln\left(\frac{N - n_{\mathrm{c}}}{n_{\mathrm{c}}}\right) + \frac{k}{e} \ln(2) + \alpha_{\mathrm{vib}}. \quad (1)$$

The first contribution is the change of the entropy-of-mixing when the density of mobile polarons is n_{c} and the density of thermally accessible sites is N. e is the magnitude of the elementary electronic charge. The second contribution is the entropy change arising from the two-fold spin-degeneracy. The final term is the high-temperature limit of the entropy change produced by a polaron altering the stiffness/frequencies of the molecular vibrations. Only the first contribution depends explicitly on carrier density. Because in our organic FETs $n_{\mathrm{c}} \ll N$ the primary contribution to the Seebeck coefficient comes from the mixing contribution. Thus, a plot of α versus the logarithm of the mobile carrier density should yield a straight line with slope $-(k/e)\ln(10) = -198$ μV/K/decade. It is evident from Fig. 2(b) that the slopes of the near-linear, experimental α-versus-log(n) plots depend on the specific polymer and exceed this value. These discrepancies can be reconciled by taking into account that a fraction f of the injected carriers n are trapped in shallow traps and do not participate in transport. Then $n_{\mathrm{c}} = n(1 - f)$ and the slope of the α-versus-log(n) plot is increased to $-(k/e)\ln(10)/(1 - f)$. This procedure is justified if these band-tail-like traps are within $\sim kT$ of the narrow band of conducting polaron states. We extract values of $f = 0.3$, 0.5 and 0.7 for IDTBT, PBTTT and PSeDPPBT, respectively. Thus, our Seebeck measurements indicate significantly less trapping in IDTBT than in PBTTT or PSeDPPBT; in IDTBT the majority of charge carriers reside in mobile states.

To interpret the magnitude of the Seebeck coefficients we estimate the number of equivalent sites in our polymers. By assuming one site on each polymer repeat unit we obtain $N = 7.4 \times 10^{20}$ cm^{-3} (IDTBT) and $N = 8.9 \times 10^{20}$ cm^{-3} (PBTTT) based on reported unit cell parameters [20, 26]. The solid red and black lines in Fig. 2(b) show the resulting estimates of the Seebeck coefficients for IDTBT and PBTTT upon ignoring the carrier-induced change of these molecules' vibrations. The small discrepancies between the solid lines of Fig. 2(b) and the experimental data may indicate the vibrational contribution. This interpretation yields 50-100 μV/K for the vibrational contribution of IDTBT. This appears reasonable, though smaller than what has been reported for pentacene (265 μV/K) [27] or boron carbides (200 μV/K at 300 K) [28].

The small degree of disorder in IDTBT is also consistent with optical absorption measurements by photo-thermal deflection spectroscopy (PDS) (SI section 8). PDS provides a bulk-sensitive method to probe energetic disorder manifesting itself as sub-bandgap tail states of the excitonic joint density of states and estimate their width in terms of the Urbach energy, E_u, extracted from the optical absorption coefficient $a(E) = a_0 \exp\left(\frac{E - E_g}{E_u}\right)$ for $E < E_g$. For more disordered polymers E_u has previously been found to correlate with the T_0 values extracted from fits of device characteristics according to an empirical relationship $E_u \approx kT_0$ [17]. Among the 20 or so, high-mobility polymers measured in this work (examples in Figs. 3 and S13) IDTBT exhibits the lowest Urbach energy of 24 meV, which is less than kT at room temperature and to the best of our knowledge the lowest value reported in a conjugated polymer. Interestingly, the second and third lowest values are also measured in high mobility polymers, naphtalenediimide-based P(NDI2OD-T2) [8,17,29] (E_u= 31 meV) and DPPTTT (E_u= 33 meV). This should be compared to PBTTT (E_u= 47 meV).

Our results demonstrate clearly that donor-acceptor copolymers without pronounced crystallinity can exhibit a lower degree of energetic disorder than (semi)crystalline conjugated polymers; it is important to understand the underlying microstructural origin for this. We are also interested in whether IDTBT's exceptional properties originate in certain, unique molecular design features that may not yet be

implemented to the same degree in other polymers with comparable mobilities, but otherwise less ideal transport characteristics. IDTBT cannot simply be understood as a classical rigid-rod polymer; already its high solubility in a wide range of solvents suggests a degree of chain flexibility that is not common for such polymers (SI section 1). To understand these questions better we have modeled the three-dimensional structures of IDTBT, P(NDI2OD-T2) and PBTTT by combining quantum-chemical and molecular dynamics (MD) calculations [30, 31] (SI section 9). The conformational search points to interdigitated side chains as the thermodynamic, lowest energy structures in the three polymers (Figure S14). However, in contrast to PBTTT [26], for IDTBT the X-ray pattern simulated for such a dense, ordered, interdigitated side chain arrangement is not in agreement with experimental data [20]. Instead, much better agreement with the measured X-ray diffraction is obtained when a less dense, disordered, non-interdigitated side chain arrangement is built from numerical annealing experiments (Figure S15). A similar protocol was also applied to simulate side-chain disorder in P(NDI2OD-T2) and PBTTT. In relation to their crystalline phases the backbone conformations in these disordered structures differ significantly between the polymers (Fig. 4(a)): IDTBT adopts a wavy, yet remarkably planar, largely torsion-free backbone; the deviation from planarity remains exceptionally small (torsion angle of 5.2° +/- 4.0°). P(NDI2OD-T2) behaves similarly; although it is not a planar molecule, the torsion angle distribution between the NDI and thiophene units remains relatively narrow (38.2° +/- 10.7°). In contrast, PBTTT chains while maintaining a linear conformation explore a broader range of torsion angles (27.2° +/- 14.6° between thiophene and thienothiophene).

We have direct experimental evidence for a near-torsion-free backbone in IDTBT from pressure-dependent Raman spectroscopy (Fig. 4(b), SI section 10). If there was significant torsion in as-deposited films the backbone could be planarized by applying a hydrostatic pressure of a few GPa, as previously observed for structurally-related poly-dioctylfluorene-co-benzothiadiazole (F8BT) [32] and the Raman intensity ratio between the ring stretching mode of the IDT unit at 1613 cm^{-1} and the ring stretching mode of the BT unit at 1542 cm^{-1} would be expected to be pressure dependent. However, we find experimentally that this ratio is remarkably pressure-independent between 0 - 2.5 GPa, suggesting that the IDTBT backbone is indeed

already planar in as-deposited films.

The frontier orbitals of the three theoretically investigated polymers are spread along the backbones (Fig. S20), so that conformational disorder is expected to broaden the density of states (DOS). We have calculated the tail width of the HOMO DOS in IDTBT to be least affected by side-chain disorder; likewise for the LUMO DOS of P(NDI2OD-T2), here partly because of the stronger confinement of the LUMO on the NDI units. In contrast, the HOMO DOS of PBTTT broadens significantly upon introducing side-chain disorder (Table 1). Remarkably, even in a completely amorphous phase simulated by cooling down low density systems made of initially highly energetic randomly distributed oligomers (SI section 9) IDTBT accommodates side-chain disorder through bends in the backbone while retaining its near planar conformation (Figure 4(c)); its DOS is not significantly broadened. In contrast, the other two polymers, in particular PBTTT, adopt conformations with a larger span in torsion angles and wider DOS. The relative trend in disorder resilience evident from Table 1 is remarkably consistent with the measured Urbach energies and transport properties.

Our results provide an explanation for the surprisingly high mobilities in donor-acceptor copolymers with less crystalline microstructure than (semi)crystalline P3HT/PBTT in terms of a low degree of energetic disorder originating in a remarkable resilience of the backbone conformation to the side-chain disorder, that is inevitable when thin films are solution-deposited by rapid drying techniques. The exceptional properties of IDTBT suggest several co-operating molecular design guidelines for discovering a wider class of such "disorder-free" conjugated polymers: (i) collinear conjugated units with only a single or minimum number of torsion-susceptible linkages in an extended repeat unit (a large size of the conjugated units will also tend to render the electronic structure less susceptible to residual torsions), (ii) a relatively steep gas-phase torsion potential with minima ideally (though not necessarily) around 180° and/or 0° (Fig. 4(d)) and (iii) long side-chain substitution on both sides of one of the conjugated units to enable space filling in non-interdigitated structures without introducing backbone torsion and hindering close $\pi-\pi$ contacts. Transport in such torsion-free polymers is approaching intrinsic limits, in which all molecular sites are thermally accessible. The level of energetic disorder as measured

by the Urbach energy is comparable to that of certain inorganic crystals, such as GaN [33]. That this is possible in near amorphous polymers is highly surprising. Our results could lead to a new generation of "disorder-free" conjugated polymers with improved charge, exciton, spin and other transport properties for a broad range of applications and observation of physical phenomena that have hitherto been prevented by disorder-induced localization.

References

[1] Bruetting, W. *Physics of Organic Semiconductors* (Wiley-VCH 2005).

[2] Baessler, H. Localized States and Electronic Transport in Single Component Organic Solids with Diagonal Disorder. *Phys. Stat. Solidi B* **107**, 9-54 (1981).

[3] Sirringhaus, H. Device Physics of Solution-Processed Organic Field-Effect Transistors. *Adv. Mater.* **17**, 2411-2425 (2005).

[4] Rivnay, J., Noriega, R., Northrup, J. E., Kline, R. J., Toney, M. F. & Salleo, A. Structural Origin of Gap States in Semicrystalline Polymers and the Implications for Charge Transport. *Phys. Rev. B* **83**, 121306 (2011).

[5] Noriega, R. *et al.* A general relationship between disorder, aggregation and charge transport in conjugated polymers. *Nat. Mat.* **12**, 1038–1044 (2013).

[6] Zhang, W. M. *et al.* Indacenodithiophene semiconducting polymers for high performance air-stable transistors. *J. Am. Chem. Soc*. **132,** 11437-11439 (2010).

[7] Nielsen, C. B., Turbiez, M. & McCulloch, I. Recent Advances in the Development of Semiconducting DPP-Containing Polymers for Transistor Applications. *Adv. Mater.* **25**, 1859-1880 (2013).

[8] Kim, N.-K., Khim, D., Xu, Y., Lee, S.-H., Kang, M., Kim, J., Facchetti, A., Noh, Y.-Y. & Kim, D.-Y. Solution-Processed Barium Salts as Charge Injection Layers for High Performance N-Channel Organic Field-Effect Transistors. *ACS Appl. Mater. Interfaces* **6**, 9614–9621 (2014).

[9] Kim, G., Kang, S.-J., Dutta, G. K., Han, Y.-K., Shin, T. J., Noh, Y.-Y., Yang, C. A thienoisoindigo-naphthalene polymer with ultrahigh mobility of 14.4 cm^2/V·s that

substantially exceeds benchmark values for amorphous silicon semiconductors. *J. Am. Chem. Soc.* **136**, 9477-9483 (2014).

[10] Tseng H.-R., Phan H., Luo, C., Wang, M., Perez, L. A., Patel, S. N., Ying, L., Kramer, E. J., Nguyen, T.-Q., Bazan, G. C., Heeger, A. J. High-Mobility Field-Effect Transistors Fabricated with Macroscopic Aligned Semiconducting Polymers. *Adv. Mat.* **26**, 2993-2998 (2014).

[11] Callen, H. B. *Thermodynamics* (Wiley, New York 1960) Chap. 17.

[12] Emin, D. "Seebeck effect," *Wiley Encyclopedia of Electrical and Electronics Engineering Online*, edited by J. G. Webster (Wiley, New York, 2013).

[13] Emin, D. Enhanced Seebeck coefficient from carrier-induced vibrational softening. *Phys. Rev. B* **59**, 6205-6210 (1999).

[14] D. Emin, *Polarons* (Cambridge University Press 2013).

[15] Pernstich, K. P., Roessner, B. & Batlogg, B. Field-effect-modulated Seebeck coefficient in organic semiconductors. *Nat. Mater.* **7**, 321-325 (2008).

[16] Kronemeijer, A. J. *et al.* A selenophene-based low-bandgap donor–acceptor polymer leading to fast ambipolar logic. *Adv. Mater.* **24,** 1558-1565 (2012).

[17] Kronemeijer, A. J. *et al.* Two-Dimensional Carrier Distribution in Top-Gate Polymer Field-Effect Transistors: Correlation between Width of Density of Localized States and Urbach Energy. *Adv. Mater.* **26**, 728-733 (2014).

[18] Chen, Z., Lee M. J., Ashraf, R. S., Gu, Y., Albert-Seifried, S., Nielsen, M. M., Schroeder, B., Anthopoulos, T.D., Heeney, M., McCulloch, I., Sirringhaus, H. High performance ambipolar diketopyrrolopyrrole-thieno[3,2-b]thiophene copolymer

field-effect transistors with balanced electron and hole mobilities. *Adv. Mat.* **24**, 647-652 (2012).

[19] Li, J., Zhao, Y., Tan H. S., Guo, Y., Di, C.-A., Yu G., Liu, Y., Lin, M., Lim, S. H., Zhou, Y. , Su, H., Ong, B. S. A stable solution-processed polymer semiconductor with record high mobility for printed transistors. *Sci. Rep.* **2**, 754 (2012).

[20] Zhang, X. *et al.* Molecular origin of high field-effect mobility in an indacenodithiophene–benzothiadiazole copolymer. *Nat. Commun.* **4**, 2238 (2013).

[21] Sirringhaus, H. Organic field-effect transistors – The path beyond amorphous silicon. *Adv. Mater.* **26**, 1319-1335 (2014).

[22] Brondijk, J. J. *et al.* Two-dimensional charge transport in disordered organic semiconductors. *Phys. Rev. Lett.* **109**, 056601 (2012).

[23] Venkateshvaran, D., Kronemeijer, A. J., Moriarty, J., Emin, D. & Sirringhaus, H. Field-effect modulated Seebeck coefficient measurements in an organic polymer using a microfabricated on-chip architecture. *APL Mat.* **2**, 032102 (2014).

[24] Germs, W. C., Guo, K., Janssen, R. A. J., Kemerink, M. , Unusual thermoelectric behavior indicating hopping to bandlike transition in pentacene *Phys. Rev. Lett.* **109**, 016601 (2012).

[25] Overhof, H., Beyer, W. A model for the electronic transport in hydrogenated amorphous silicon. *Phil. Mag. B* **43**, 433-450 (1981).

[26] DeLongchamp, D. M. *et al.*, High Carrier Mobility Polythiophene Thin Films: Structure Determination by Experiment and Theory. *Adv. Mater.* **19**, 833-837 (2007).

[27] Muehlenen, A., Errien, N., Schaer, M., Bussac, M.-N. & Zuppiroli, L. Thermopower measurements on pentacene transistors. *Phys. Rev. B* **75**, 115338 (2007).

[28] Aselage, T. L., Emin, D., McCready, S. S., & Duncan, R. V. Large Enhancement of Boron Carbides' Seebeck Coefficients through Vibrational Softening. *Phys. Rev. Lett.* **81**, 2316-2319 (1998).

[29] Yan, H., Chen, Z., Zheng, Y., Newman, C., Quinn, J. R., Dötz, F., Kastler, M., Facchetti, A. A high-mobility electron-transporting polymer for printed transistors. *Nature* **457**, 679-686 (2009).

[30] Olivier, Y., Niedzialek, D., Lemaur, V., Pisula, W., Müllen, K., Koldemir, U., Reynolds, J.R., Lazzaroni, R., Cornil, J., Beljonne, D**.** High-Mobility Hole and Electron Transport Conjugated Polymers: How Structure Defines Function. *Adv. Mat.* **26**, 2119-2136 (2014).

[31] Cho, E., Risko, C., Kim, D., Gysel, R., Miller, N. C., Breiby, D. W., McGehee, M. D., Toney, M. F., Kline, R. J. & Jean-Luc Bredas. Three-Dimensional Packing Structure and Electronic Properties of Biaxially Oriented Poly(2,5-bis(3-alkylthiophene-2-yl)thieno[3,2-*b*]thiophene) Films. *J. Am. Chem. Soc.* **134** (14), 6177-6190 (2012).

[32] Schmidtke, J.P., Kim, J.-S., Gierschner, J., Silva, C., Friend, R. H. Optical Spectroscopy of a Polyfluorene Copolymer at High Pressure: Intra- and Intermolecular Interactions. *Phys. Rev. Lett.* 99, 167401 (2007).

[33] Jacobson, M. A., Konstantinov, O. V., Nelson, D. K., Romanovskii, S. O. & Hatzopoulos, Z. Absorption spectra of GaN: film characterization by Urbach spectral tail and the effect of electric field. *Journal of Crystal Growth* **230***,* 459-461 (2001).
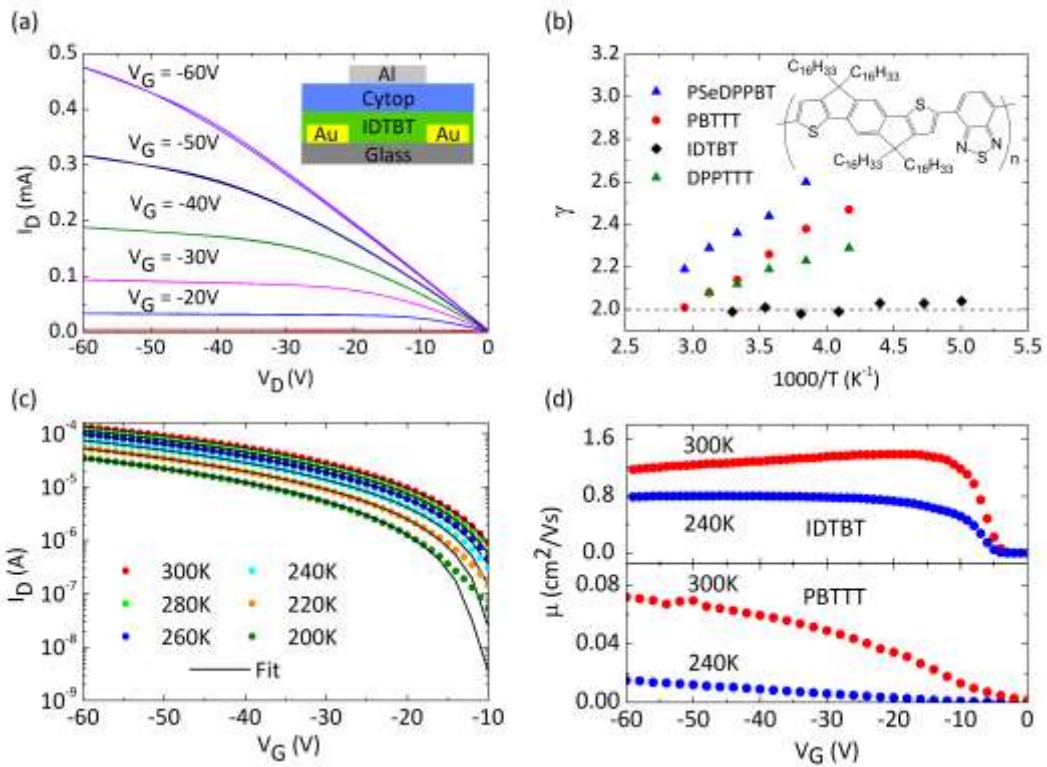
Figure 1 Transistor characteristics of IDTBT-based FETs compared with other polymer FETs. (a) Room-temperature output characteristics and device architecture of a typical IDTBT OFET with L = 20 μm and W = 1 mm. (b) γ plotted versus 1000/T for IDTBT (structure shown), PSeDPPBT, DPPTTT and PBTTT OFETs. (c) Temperature evolution of IDTBT transfer curves fitted with a disorder-free MOSFET model (V_D = -60 V). (d) Gate-voltage dependence of saturation mobility at 300 K and 240 K for patterned IDTBT (top) and PBTTT (bottom) devices.
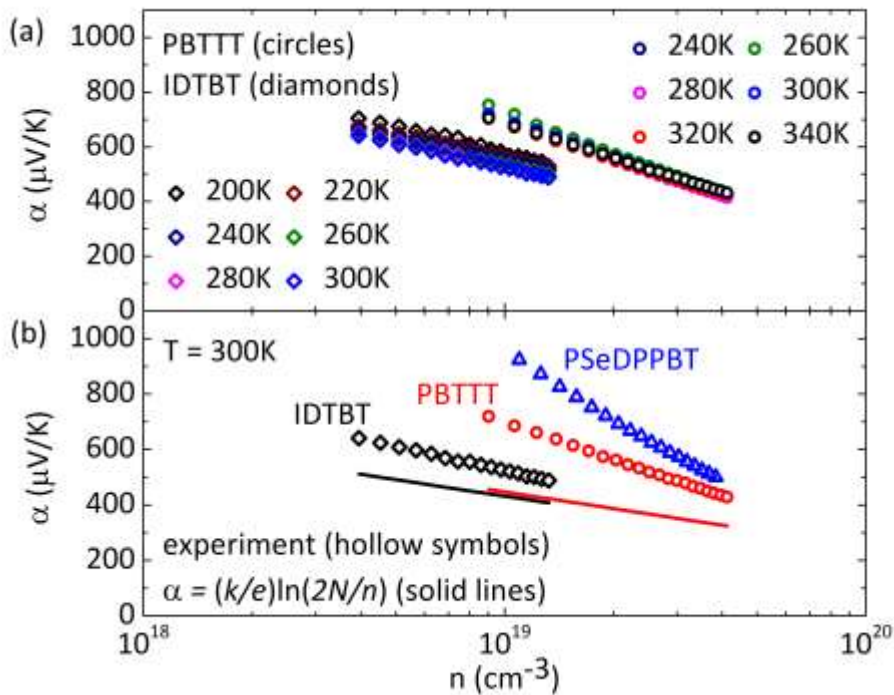
Figure 2 Field-effect modulated Seebeck coefficients in high mobility polymer devices. (a) Temperature independence of the field-effect modulated Seebeck coefficient of PBTTT and IDTBT. (b) Slopes of the Seebeck coefficients versus the logarithm of carrier concentration in the accumulation region for IDTBT, PBTTT and PSeDPPBT at 300 K. The solid lines in (b) are plots of $\alpha = (k/e)\ln(2N/n)$. The carrier concentration in IDTBT is slightly lower than in the other polymers because of the low-k Cytop gate dielectric used. The measurement error of the Seebeck coefficient is estimated to be ± 70 µV/K for the IDTBT device (SI section 2).
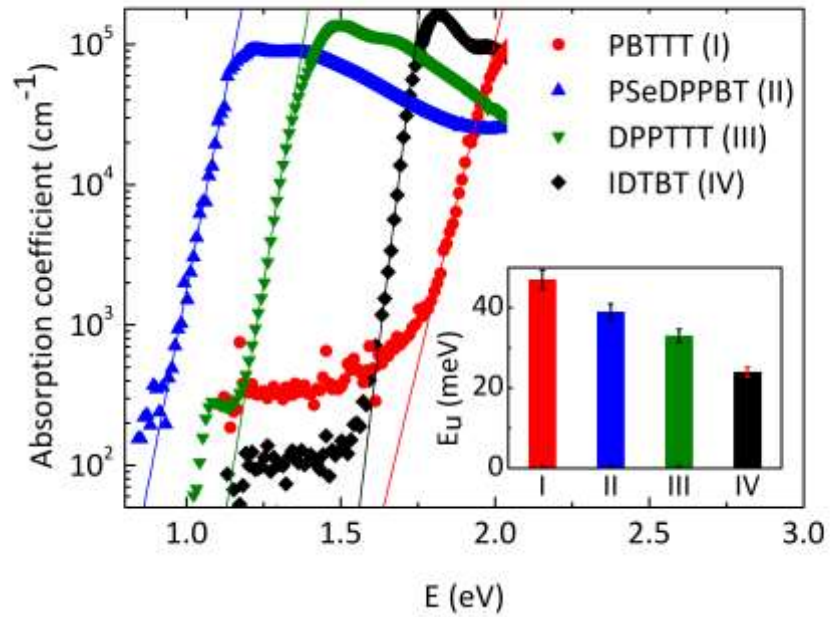
Figure 3 Energetic disorder probed using Photothermal Deflection Spectroscopy. Absorption coefficient of IDTBT, DPPTTT, PSeDPPBT and PBTTT films, measured by Photothermal Deflection Spectroscopy. Solid lines represent exponential tail fits for extraction of the Urbach energies E_u. A relative error of 5 % in the value of E_u was estimated due to uncertainty in the fitting procedure.
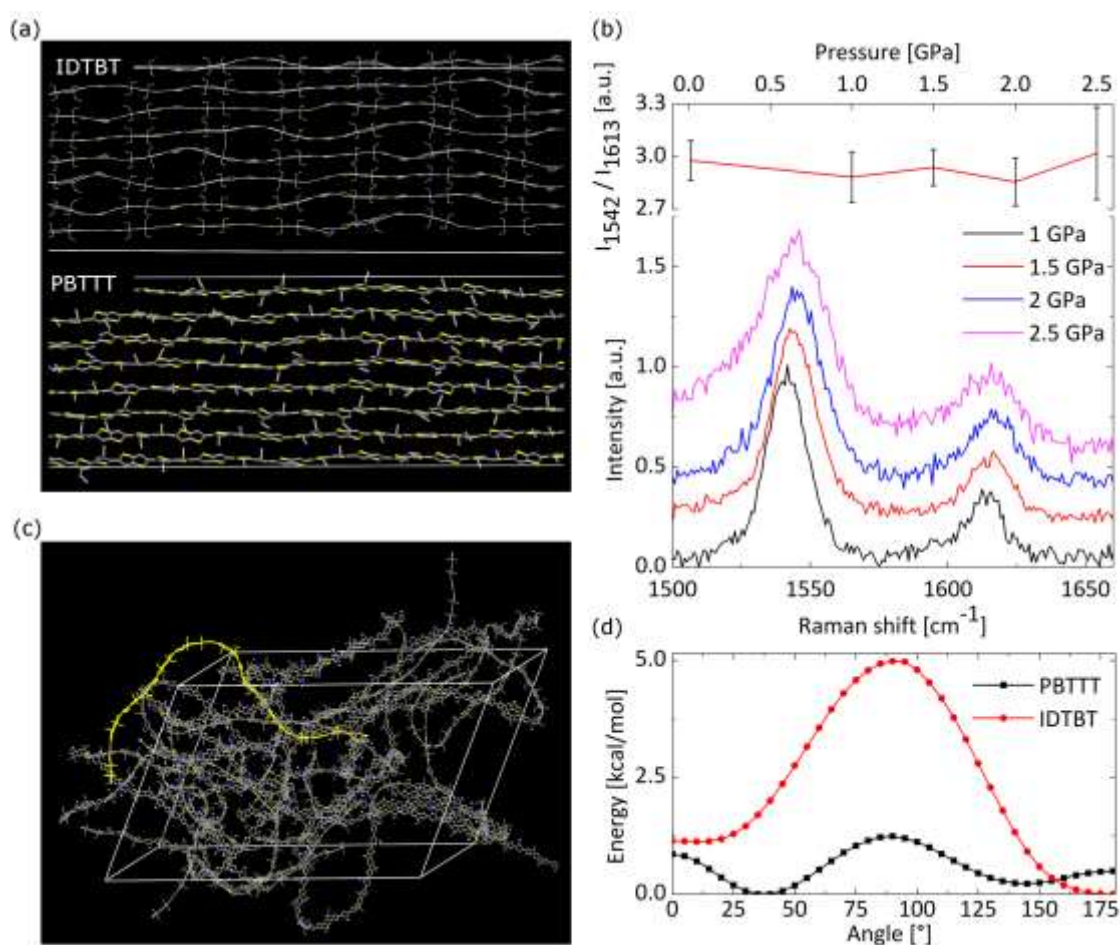
Figure 4 Resilience of torsion-free polymer backbone conformation to side-chain disorder. (a) Simulations of the backbone conformation of IDTBT and PBTTT in side-chain disordered and non-interdigitated structures. The side chains and hydrogen atoms are omitted for clarity. (b) Pressure dependence of the Raman spectrum of IDTBT measured using a diamond anvil cell. (c) Simulation of the backbone conformation of IDTBT in the amorphous phase. A single chain from the simulated unit cell has been highlighted. (d) Calculated gas phase torsion potentials of IDTBT and PBTTT. For PBTTT the potential for torsion between the thiophene and thienothiophene units is shown.

	IDTBT HOMO (meV)	P(NDI2OD-T2) LUMO (meV)	PBTTT HOMO (meV)
Crystalline	26	33	30
Disordered	31	44	48
Amorphous	31	69	108

Table 1 Side chain disorder induced broadening of the density of states. Values of the width of the tail of the density of states extracted by fitting the simulated density of states of the different polymers/phases to an exponential function.

Competing financial interests

The authors declare no competing financial interests.

Author Contributions

DV designed, fabricated and performed measurements on the devices for field-effect modulated Seebeck measurements. MN and AJK optimized the fabrication of IDTBT based OFETs and performed transistor measurements. AS and MN performed PDS measurements. VP optimized the patterning procedure for organic devices. VL, MZ, YO, JC and DB performed quantum chemical and molecular dynamic simulations. MZ and MK acquired the high-pressure induced Raman spectra. KB performed measurements on DPPTTT based devices. IN and IR performed Charge Accumulation Spectroscopy measurements shown in the Supplementary Information. IM and MH synthesized IDTBT. DE explained the Seebeck measurements based on a narrow band model. HS directed and coordinated the research. DV, MN, VL, DE and HS wrote the manuscript.